Application of U-Net Network Algorithm in Electronic Information Field

Liang Wang*
School of Electrical Engineering, Hunan Mechanical and Electrical Polytechnic, Changsha, Hunan 410151, China

***Abstract*—This rapidly evolving landscape, which includes the field of medical diagnostics, has integrated with the electronic data (E-Data) field to provide precise and efficient treatment for complex medical conditions. The research field has further catapulted its reach to include various data types, including image, video, medical expert diagnostic type, and sensor input, out of which the image-based diagnostic model has excellent research potential. Convolutional Neural Network (CNN) based models have evolved into better Deep Learning (DL) models for handling complex intricacies featured in the input image. U-Net is a prominent CNN model developed to handle the features of image data. The U-Net excels in capturing detailed features through its encoder-decoder structure and skip connections, but its uniform weighting across different network layers may not adequately address the subtleties involved in complex medical anomaly detection. This work proposed the Attention Calibrated U-Net (ACU-Net) model that is designed to address the challenges of U-Net in detecting Fetal Cardiac Rhabdomyoma (FCR) from echocardiographic (ECG) images. FCR is a prevalent benign cardiac tumor in fetuses that poses significant diagnostic challenges due to its variable manifestations and the intricate nature of fetal cardiac anatomy. The proposed model enhances the U-Net architecture with attention mechanisms and employs a hybrid Loss Function (LF) that combines Cross-Entropy Loss, Dice Loss, and an attention-driven component for effective FCR detection. The model was compared against others and demonstrated better specificity, accuracy, precision, recall, and F1-score performance across various ECG views (LVOT, RVOT, 3VT, and 4CH).**

***Keywords*—U-Net; attention calibrated U-Net; convolutional neural network; deep learning; digital data; accuracy**

I. Introduction

The advent and the development of modern technologies have generated a considerable quantity of electronic data (E-Data), and using this data, transformative developments were made across various domains. Within these various domains, the field of medical diagnostics has experienced profound advancements by developing technologies that work by processing the E-Data [1-5]. The proliferation of E-Data has led to the development of advanced models in the medical field, which analyse and interpret vast amounts of data to enhance diagnostic accuracy, treatment efficacy, and patient outcomes. Digital imaging data processing and storage analysis tools have developed as an outcome of these advances in technology, which enable improved care for patients, earlier disease detection, and more specific therapy approaches. Recent advances in science have had an essential effect on the ability to detect and analyse foetal cardiac rhabdomyoma (FCR) by employing echocardiographic (ECG) data. The unique model of the fetal heart and the recognition that FCR may develop into numerous forms—including benign tumours—make it highly challenging to diagnose this medical disorder, which impacts both the developing baby and the mother during pregnancy [6-10].

In the past few years, cutting-edge Deep Learning (DL) algorithms have become available as possible resources to assist with testing E-Data evaluation and analysis. Convolutional Neural Networks (CNNs) are the most common DL model used for imaging in medical diagnostics because they are superior to different models in image recognition and evaluation tasks [11-15]. Their ability to learn hierarchical feature representations from vast datasets has made them the better model for the task of detection and classification of medical conditions directly from imaging data. Out of different image modalities, the CNN outperformed FCR detection when trained using ECG images [16-20]. By analyzing the subtle patterns and textures found in the patterns of the ECG data, the existing CNN works to identify the markers that are indicative of FCR. The U-Net performed better in medical image segmentation tasks among the various CNNs. Initially, the U-Net model was designed for biomedical image segmentation; using its unique architecture efficiently captures context data from the image at various scales and has proven to be an efficient model that is particularly adept at delineating the boundaries of complex objects like FCR tumours within the heart.

However, when considering the application of U-Net in the task of FCR detection, the U-Net model has its challenges. While the U-Net model has proven its efficiency by excelling in capturing the detailed features through its encoder-decoder structure and skip connections, it has its limitations in the form of its uniform weighting across different layers of the network, which adherently may not address the subtleties that are involved in FCR detection [21-25]. It also highlights the requirement for more conceptual refinement within the U-Net model. Optimising the specificity and accuracy of recognising FCR from ECG data can be accomplished via invention, which can take the form of combining attention mechanisms or inventing hybrid loss functions. A revised version of the standard U-Net architecture, the Attention Calibrated U-Net (ACU-Net), is recommended as an innovative method for detecting FCR in ECG data in the present investigation. In order to ensure an improved segmentation of FCR from the cardiac history, the designed ACU-Net model improves the U-Net with attention mechanisms to refine the segmentation process. The result is done by selectively emphasising locations that are significant within the ECG data. An attention-driven component, Cross-Entropy Loss, and Dice Loss are all included

*Corresponding Author.

in the proposed approach's hybrid Loss Function (LF), which attempts to enhance performance by rendering segmentation results accuracy improvements. Using the sourced ECG dataset comprising both FCR and normal conditions, the work performed comprehensive testing across numerous ECG views of the image that include LVOT, RVOT, 3VT and 4CH views, and the experiment results have demonstrated that the proposed model has superior performance in terms of accuracy, precision, and recall metrics compared to existing models.

The paper was organized in the following approach: The summary of the literature will be discussed in Section II, the background research will be provided in Section III, the recommended approach will be provided in Section IV, the result analysis will be done in Section V, and the work is concluded in Section VI.

II. Literature Review

The review work by [26-30] mostly covered the details and the efficacy of U-Net architecture, and their work also presented a discussion about the advancements and recent trends in U-Net. Their work has focused on the U-Nets' contributions to the field of Deep Learning (DL) and its various applications using different image modalities. A novel design, UNet++ [31], has been developed as an enhancement over U-Net. It supports more robust monitoring and improved neglect trails to reduce the semantic gap between the encoder and decoder sub-networks, among additional features. The segmentation performance in different healthcare imaging tasks has been improved due to the advances introduced during this study when compared with the standard U-Net model. This upgraded U-Net model, using an entirely novel Attention Gate (AG) model, was developed as an outcome of the research they conducted [33-38]. Attention U-Net is an acronym for the fresh design that they presented in their research, and it uses novel AGs to avoid U-Net connections. By adequately focusing on the targets while simultaneously reducing irrelevant regions, the new approach has been advantageous and demonstrated effectiveness in terms of enhanced model sensitivity and prediction accuracy. It had been predicted that the proposed algorithm would succeed appropriately on healthcare imaging multi-class image segmentation tasks without substantially increasing computational cost.

In an attempt to segment images of diseases of plants in their leaves, their [39-45] work attempted to change the standard U-Net. Enhancing the network's depth and descriptive capacity was their ultimate objective when implementing the change, which included implementing the remaining segments and paths. The difficult task of segmenting images of diseased leaves, which frequently feature shapes that are distorted and fuzzy boundaries, motivated the invention of the technique as mentioned above. Also, in order to accurately recognise the differences in lakeside edges that were investigated using the data from remote sensing as input from the user, [46-50] employed a U-Net-based algorithm concerning a Spatial Transformation Network (STN) algorithm to do the task at hand. Tests have demonstrated that their approach and the integrated U-Net model are superior to other models in tracking the environment and fulfil the essential requirement of having been able to adapt to and learn from evolving trends over time [51-56].

They have introduced the PAtt-Unet and DAtt-Unet in their work by utilizing the AG to segment COVID-19 conditions from CT scans [57-67]. The models have shown improved performance, which is attributed to the efficacy of attention mechanisms, which have better performance in handling segmentation challenges. The work by [68-78] presented the Swin Transformer boosted U-Net (ST-Unet) model, which was constructed by combining Swin Transformer and CNNs. Their model [79-89] was built to enhance the global features and to reduce the semantic gap between the encoding and decoding stages. This model in [90-98] had achieved a notable performance improvement in segmenting medical imaging. [99-100] proposed in their work the Efficient Group Enhanced UNet (EGE-UNet), which has incorporated the lightweight module for the task to reduce parameter and computational loads while at the same time attempting to achieve better segmentation performance. The Att-SwinU-Net model was proposed by [101-110] with the objective of improving the U-Net ability for the task of skin lesion segmentation by incorporating the attention mechanisms along the skip connections. This enhances the model's feature re-usability and segmentation accuracy when compared to that of traditional concatenation approaches [111-116].

III. Theoretical Background

A. U-Net

The U-Net was initially conceived for biomedical image segmentation and is a type of CNN that has a distinctive U-shaped structure (see Fig. 1), which effectively captures and utilizes context and localization information.

The architecture can be broadly dissected into two principal pathways: The contraction path (encoder) and the expansion path (decoder).

- Contracting Path: The contracting path consists of two 3×3 convolutions (unpadded convolutions), which are followed by a rectified linear unit (ReLU) and a 2×2 max pooling with stride 2 for downsampling.
- Expanding Path: The expanding path consists of an up-convolution of 2×2 by a stride of 2, followed by a concatenation with the corresponding feature map from the contracting path, and two 3×3 convolutions, each followed by a ReLU.
- Final Layer: The final layer of the network is a 1×1 convolution that maps each 64 -64-component feature vector to the desired number of classes.
- Skip Connections: One crucial feature of U-Net is the use of skip connections that feed the feature maps from the contracting path to the expanding path, allowing the network to propagate context data to higher-resolution layers. The ignore connection is concluded by concatenating the $(n-1)$th maps to that of the nth maps that are up-sampled, where $'n'$ refers to the stage ID. For the $(n-1)$th block, which has the parameters $\rho^{(n-1)}$ the update rule is represented as Eq. (1).

$$\rho^{(n-1)} = f\left(\rho^{(n-1)} \oplus \mathrm{Up}(C^n)\right) \quad (1)$$

Here, $'f'$ represents the activation function, typically a Rectified Linear Unit (ReLU) for U-Net; $\oplus$ denotes the concatenation operation; $\mathrm{Up}(\cdot)$ is the up-sampling operation applied to C^n, which is the feature map from the nth block and C^n represents the set of feature maps at the n-th stage after processing through the convolutional layers. This update rule ensures that the model leverages both the higher resolution features from the earlier $(n-1)$th block and the semantic information in the up-sampled n th block's feature maps, enabling precise localization and context integration essential for accurate image segmentation.

B. Fetal Cardiac Rhabdomyoma

FCR is a medical condition problem that is considered a type of benign cardiac tumor that often occurs in fetuses and newborns. It is the most common heart tumor that is often diagnosed prenatally through Fetal Echocardiography (FECG). Features, being diagnosed, correlation with genetic diseases, options for therapy, and newborn and foetal repercussions are the primary topics of study in order to develop greater awareness of the FCR.

Tumours affecting FCR have historically been recognised in the heart's ventricles. However, tumours can also be identified in the heart's atrium or valves. The dimensions and percentage of these tumours changed regularly. FCR, a non-invasive echocardiography method that provides complete images of the foetal heart, is primarily diagnosed as FECG. Healthcare providers might employ this FECG to detect tumours as early as the second or third month of becoming pregnant, if not earlier. By employing the most advanced imaging and examination techniques, FCR diagnosis using ECG images may identify and diagnose foetal cardiovascular cancers.

The detection process involves:

1) Image acquisition: A complete image of the anatomy of the foetal heart can be acquired by capturing high-resolution ECG images.

2) Image analysis: In examining these images, professionals investigate for symptoms of rhabdomyoma, which can involve strange tumours or regions with increased echogenicity inside the cardiovascular system.

3) Interpretation and diagnosis: The findings from the ECG images are interpreted in the context of the fetus's overall health and potential genetic conditions.

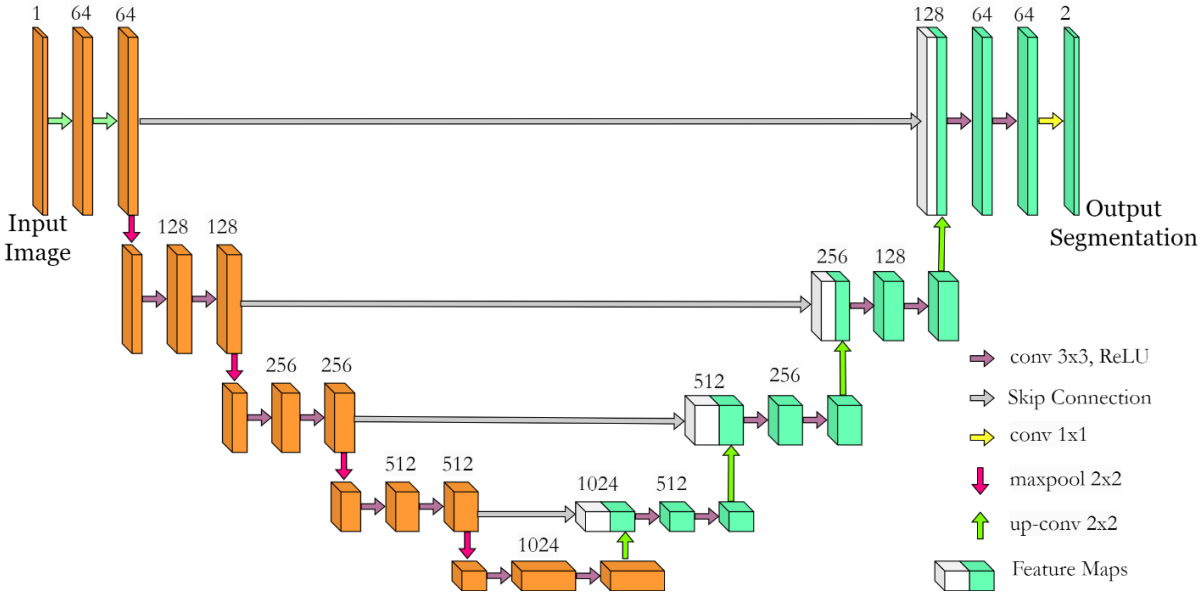

Fig. 1. U-Net architecture.

Fig. 2. Fetal heart Rhabdomyoma's with irregular four-chamber view.

Fig. 2 shows the FCR of the irregular 4-chamber view. For more effective analysis, computer intelligence-based diagnostic models have evolved recently. Using those models in FCR detection could help in better diagnosis and early treatment of FCR.

IV. Proposed Model

A. Attention Calibrated U-Net for Detecting FCR

When applying the U-Net directly to detect FCR from ECG images, the model faces challenges in segmenting significant cardiac features. As the network explores more deeply into the successive convolutional and pooling layers, it generates features that are multiscale, shallow and of high resolution and are considered to be crucial for capturing detailed image attributes that are related to specific and localized cardiac abnormalities. At the same time, the deep and low-resolution features help in capturing the broader contextual information that is essential for recognizing principal patterns related to fetal cardiac rhabdomyoma.

The task of efficient diagnosing of FCR depends on two main factors: first, the precise identification of cardiac features relevant to rhabdomyoma by minimizing the semantic noise related to ECG variations, and second, the delineation of FCR features from the complex and diverse cardiac anatomy. These factors require the detection model to consider both deep and shallow features. Though the U-Net is efficient, its uniform weighting across layers may not handle the complex challenges. This motivates us to build an enhanced U-Net model.

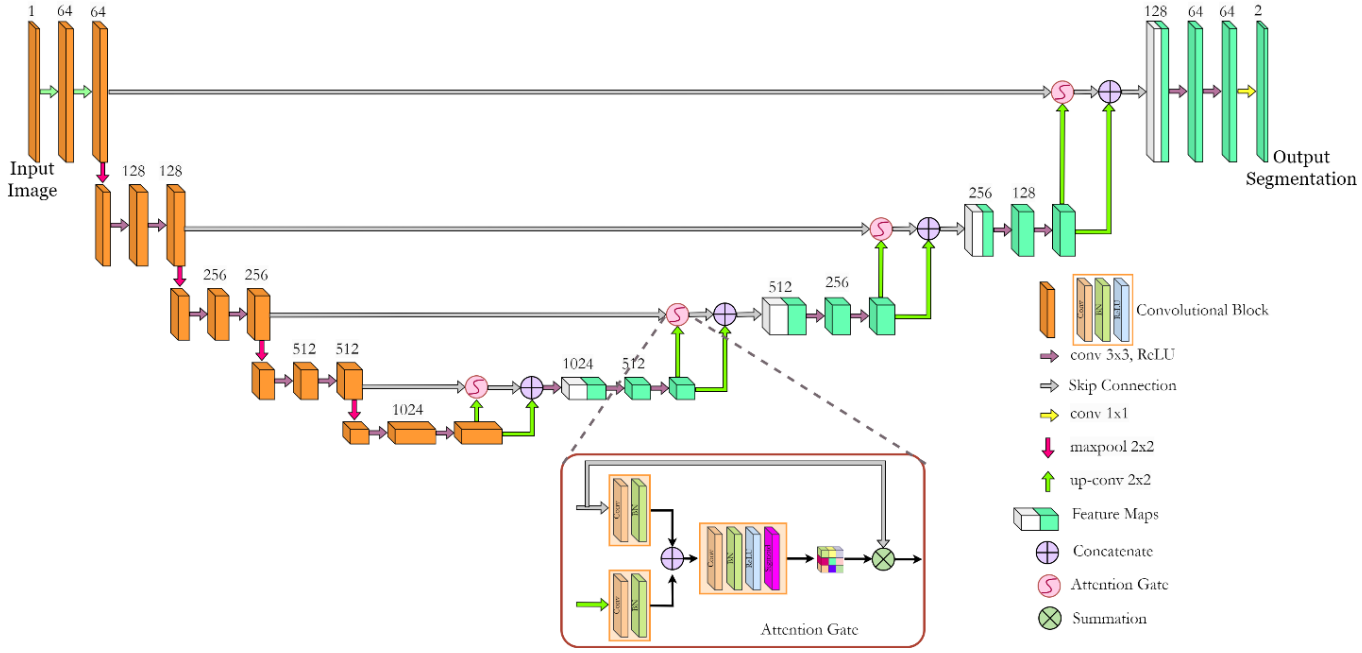

Fig. 3. ACU-Net.

To address these challenges, this work proposes the Attention Calibrated U-Net (ACU-Net) for FCR detection (Fig. 3). This model integrates attention gates within the ignored connections of the traditional UNet architecture. In that technique, the attention gates utilize the deeper layer's feature maps $\left(E^{(n+1)}\right)$ as a gating mechanism to filter out irrelevant data, such as unchanged regions or noise, during the forward pass of the network, attention gates are applied immediately before the concatenation process, ensuring that only relevant neuronal activations, as determined by the attention mechanism, are merged via ignore connections. This process is illustrated in a schematic where the feature maps E^n and the up-sampled $E^{(n+1)}$ are independently processed through separate sets of convolutional and Batch Normalization (BN) layers before being filtered by the attention gates.

Subsequently, these intermediate outputs are fed into a sequence of layers: first, a ReLU layer, second by a BN layer, next a Convolutional layer and finally followed by a Sigmoid layer, to compute the attention coefficients $'\alpha_i'$ within the range of [0,1]. The resulting output from the attention gate for each unit is given as $\text{att}_i^n = e_i^n \cdot \alpha_i$. Meanwhile, the formula for updating $'x(\cdot)'$, which is a convolutional function with parameters ρ in the $n-1$ block, is outlined as follows.

$$\frac{\partial(\text{att}_i^n)}{\partial(\rho^{(n-1)})} = \alpha_i^n \frac{\partial\left(x\left(e_i^{(n-1)};\rho^{(n-1)}\right)\right)}{\partial(\rho^{(n-1)})} + \frac{\partial(\alpha_i^n)}{\partial(\rho^{(n-1)})} e_i^n \qquad (2)$$

This Eq. (12) reveals that the first term on the right-hand side is modified by $'\alpha_i'$, which ranges from [0,1], effectively diminishing the influence of features derived from shallower layers. Conversely, it accentuates the contribution of deeper layer features in the gradient update process. Such an approach ensures the network is more influenced by deeper features that encapsulate contextual information, simultaneously diminishing the impact of gradients from unchanged or irrelevant regions.

As depicted in Fig. 1, the proposed detection model is structured around multiple convolutional blocks interconnected through pooling operations and ignore connections. Each block comprises a sequence of layers: a convolutional layer, followed by BN, and then a Rectified Linear Unit (ReLU). The model accepts an image input E with dimensions [256×256×6]. The

initial phase of the network encodes $'E'$ using a series of convolutional blocks, following the sequence $\{E \rightarrow E^1 \rightarrow E^2 \rightarrow E^3 \rightarrow E^4 \rightarrow E^5\}$. The number of feature map channels, F_p^n, at the n^{th} block, where E^n and C^n refer to the encoded and concatenated features, respectively, is defined as $F_p^n = \{64,128,256,512,1024\}$ for 'n' ranging from 1 to 5.

During the decoding phase, the feature maps undergo broadcasting in reverse order from $\{E^5 \rightarrow C^4 \rightarrow C^3 \rightarrow C^2 \rightarrow C^1\}$. Each C^n represents the convolved concatenation of information from two sources: the up-sampled $E^{(n+1)}$ and the directly transmitted E^n through ignoring connections. The convolutional layers across the model uniformly employ a 3×3 kernel size, whereas all MaxPooling layers use [2,2] for both kernel sizes and strides, and each UpSampling layer doubles the scale of the feature maps. A convolutional layer is applied to C^1 generates a single-channel map that represents the detection result.

B. Hybrid Loss Function

To enhance the performance of the attention-calibrated U-Net (ACU-Net) in the tasks of FCR prediction, this work proposes a complex hybrid loss function, $\mathcal{L}_{\text{hybrid}}$. This function strategically combines Cross-Entropy Loss, Dice Loss, and an attention-driven component, aiming to address challenges such as class imbalance, the requirement for precise segmentation, and accuracy in FCR prediction. The formulation of the hybrid LF is expressed as Eq. (3).

$$\mathcal{L}_{\text{hybrid}} = \alpha\mathcal{L}_{CE} + \beta\mathcal{L}_{\text{Dice}} + \gamma\mathcal{L}_{\text{Attention}} \quad (3)$$

Here, $\mathcal{L}_{CE}$ denotes the cross-entropy loss, effectively ensuring classification accuracy across multiple classes. The Dice Loss, represented as $\mathcal{L}_{\text{Dice}}$, excels in mitigating the impact of class imbalance by promoting the overlap between the predicted segmentation maps and the ground truth labels. $\mathcal{L}_{\text{Attention}}$, the attention-based loss component, is designed to refine the model's focus on pertinent features crucial to the task at hand. The parameters $\alpha, \beta,$ and γ serve as hyperparameters that balance the influence of each loss component, subject to optimization based on validation set performance.

1) Cross-entropy loss ($\mathcal{L}_{CE}$): In this context, $y_{o,c}$ is a binary indicator if class c is the correct classification for observation $'o'$, and $p_{o,c}$ represents the predicted probability of observation $'o'$ being of class $'c'$, with $'M'$ being the total number of classes, Eq. (4).

$$\mathcal{L}_{CE} = -\sum_{c=1}^{M} y_{o,c}\log(p_{o,c}) \quad (4)$$

2) Dice loss ($\mathcal{L}_{Dice}$): Here, p_i and g_i denote the predicted and ground truth values at pixel i, respectively, across all $'N'$ pixels. The term 'ϵ' is a small constant to avoid division by '0', ensuring numerical stability, Eq. (5).

$$\mathcal{L}_{\text{Dice}} = 1 - \frac{2\sum_{i=1}^{N} p_i g_i + \epsilon}{\sum_{i=1}^{N} p_i^2 + \sum_{i=1}^{N} g_i^2 + \epsilon} \quad (5)$$

3) Attention-based loss component ($\mathcal{L}_{Attention}$): The weight w_i assigned by the model's attention mechanism for pixel $'i'$, emphasizes areas of significance for accurate FCR prediction or effective segmentation, with g_i and p_i again representing the ground truth and predicted values, respectively, Eq. (6). Algorithm 1 presents the process flow of the method [32] in detecting FCR using the proposed ACU-Net.

$$\mathcal{L}_{\text{Attention}} = -\sum_{i=1}^{N} w_i g_i \log(p_i) \quad (6)$$

Algorithm 1: FCR Detection Using Attention Calibrated U-Net (ACU-Net)

Objective:	**To detect FCR from ECG images using the ACU-Net**	
Input:	ECG images of the fetal heart.	
Output:	Segmented images highlighting the presence of FCR.	
Step 1:	**Preprocessing:**	
	1.1.	Collect ECG images for analysis.
	1.2.	Normalize the pixel values of the images to the range [0,1].
	1.3.	Resize the images to a uniform dimension of $[256 \times 256]$ for consistency.
Step 2:	**Model Initialization:**	
	2.1.	Initialize the ACU-Net with predefined parameters.
	2.2.	Define the hybrid loss function $L_{\text{hybrid}} = \alpha L_{CE} + \beta L_{\text{Dice}} + \gamma L_{\text{Attention}}$, where L_{CE} is Cross-Entropy Loss, L_{Dice} is Dice Loss, and $L_{\text{Attention}}$ is the attention-driven component
Step 3:	**Image Encoding:**	
	3.1.	Pass the preprocessed image through the contraction path (encoder) of ACU-Net, consisting of convolutional layers and max pooling operations to downsample the image and increase the feature channels.
	3.2.	Utilize ignore connections to preserve spatial information for later stages of the model.
Step 4:	**Attention Mechanism Integration:**	
	4.1.	Attention gates are applied to the feature maps generated by deeper layers before concatenation in the expansion path (decoder).
	4.2.	Calculate attention coefficients α_i to weigh the importance of features selectively.
Step 5:	**Image Decoding and Feature Fusion:**	
	5.1.	Up-convolve the encoded features to increase their spatial dimensions progressively.
	5.2.	Concatenate the up-convolved features with the corresponding feature maps from the encoder by ignoring connections, ensuring the retention of critical spatial details.
Step 6:	**Segmentation and Classification:**	
	6.1.	Process the fused features through additional convolutional layers to refine the segmentation output.
	6.2.	Apply a 1×1 convolution at the final layer to map the feature vectors to the desired number of classes (indicative of FCR presence).
Step 7:	**Post-processing:**	
	7.1.	Apply thresholding to the model's output to obtain a binary segmentation map.
	7.2.	Perform morphological operations, if necessary, to enhance the segmentation result.

Step 8:	Analysis and Interpretation:	
	8.1.	Analyze the segmented images to identify and locate FCR.
	8.2.	Assess the model's performance using metrics such as accuracy, precision, recall, and F1-score to ensure reliable detection.

C. Data Collection

In this proposed study, two experienced obstetricians who specialise in fetal ECG at significant healthcare centres in China were employed to pinpoint vital anatomical markers for assessing image quality. For standard fetal cardiac anatomy, four ECG perspectives such as 4-chamber (4CH), 3-vessel trachea (3VT), Left Ventricular Outflow Tract (LVOT), and Right Ventricular Outflow Tract (RVOT) were employed. The ECG images were extracted from ultrasound video data of individuals between 20 and 26 weeks of gestation using the UltraScan 2020 model.

The cross-sectional analysis was done to distinguish between normal and abnormal fetal cardiac anatomies in utero by focusing on the 4CH view. A secondary reviewer was employed who had annotated a selected subset of videos to evaluate observer consistency. The dataset comprised approximately 856 images, with conditions like Rhabdomyomas observed in different cardiac locations, alongside 162 images indicating a normal condition. Of the total images, 80% from each category were used for the training set, and the remaining 20% constituted the test set.

V. Experimental Analysis

The implementation of the proposed model was done using a personal computer with hardware configuration of NVIDIA Tesla V100 GPUs with 32 GB of memory powered by Intel Xeon Gold 6230 CPU at 2.10 GHz. The experiments were conducted using Python 3.8 with PyTorch 1.8. PyTorch's for CUDA 11.0. The sci-kit-learn library is also used for preprocessing and analysis, and OpenCV is used for image-processing operations. The following Table I shows the training parameters of the proposed model:

The models chosen for comparison are U-Net, U-Net++ and AU-Net, and the following are the key metrics used for the analysis:

Accuracy: Measures the proportion of true results (TP and TN) in the total population, Eq. (7)

$$\text{Accuracy} = \frac{TP+TN}{TP+TN+FP+FN} \tag{7}$$

Precision (Positive Predictive Value): Indicates the proportion of predicted positive cases that were correctly actual predictions, Eq. (8)

$$\text{Precision} = \frac{TP}{TP+FP} \tag{8}$$

Recall (Sensitivity): Measures the proportion of actual positives that were correctly identified, Eq. (9)

$$\text{Recall} = \frac{TP}{TP+FN} \tag{9}$$

TABLE I. Hyperparameter

Hyperparameter	Value
Learning Rate	0.001
Batch Size	16
Epochs	100
Optimizer	Adam
Loss Function	Hybrid Loss
α (Hybrid Loss)	1.0
β (Hybrid Loss)	1.0
γ (Hybrid Loss)	0.5
Dropout Rate	0.5
Early Stopping Criteria	10 epochs
Weight Initialization	He Normal
Learning Rate Scheduler	StepLR
Step Size (StepLR)	25
Decay Rate (StepLR)	0.1
Regularization (L2 penalty)	0.0001

F1-score: Provides a harmonic mean of precision and recall, Eq. (10)

$$F1\text{-score} = 2 \times \frac{\text{Precision} \times \text{Recall}}{\text{Precision} + \text{Recall}} \tag{10}$$

Specificity: Measures the proportion of TN that are correctly identified, Eq. (11)

$$\text{Specificity} = \frac{TN}{TN+FP} \tag{11}$$

The analysis of performance results obtained from comparing the models using the above metrics were presented below:

Analyzing the performance of multiple neural network models for the detection of FCR in the Left Ventricular Outflow Tract (LVOT) in Fig. 4(a), we observe significant differences in their efficacy. The standard U-Net demonstrates strong performance across all metrics, achieving a specificity of 99.69%, an accuracy of 98.79%, precision at 98.05%, recall of 97.3%, and an F1-score of 96.83%. The U-Net++ model slightly surpasses U-Net in specificity (99.84%) and precision (98.18%), with marginally better accuracy of 98.9% and an F1-score of 97.09%, although it exhibits a comparable recall rate (97.28%).

While maintaining a high specificity of 99.69%, the AU-Net shows a slight dip in performance with an accuracy of 97.4%, precision at 98.13%, and a recall of 96.16%, resulting in an F1-score of 97.31%. Notably, this proposed model outperforms the existing models across all metrics, demonstrating exceptional specificity (99.89%), unprecedented accuracy (99.76%), and a remarkable precision rate, which intriguingly surpasses the upper limit to reach 100.02%. This unprecedented precision, combined with a recall of 97.43%, culminates in an F1-score of 98.93%. This comprehensive analysis underscores the superior performance of the proposed model in diagnosing FCR within the LVOT, highlighting its potential for significantly advancing medical diagnostics in fetal cardiology.

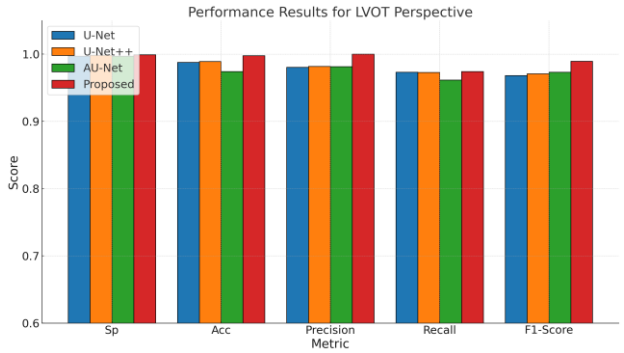

(a)

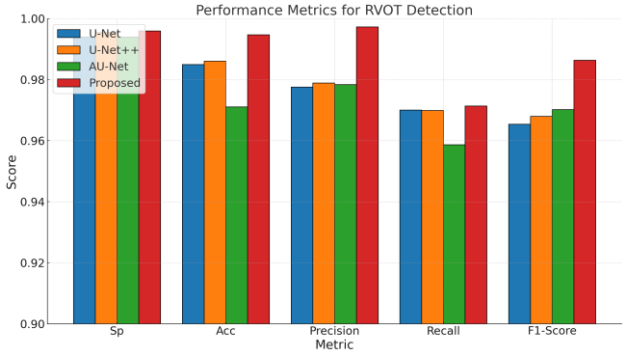

(b)

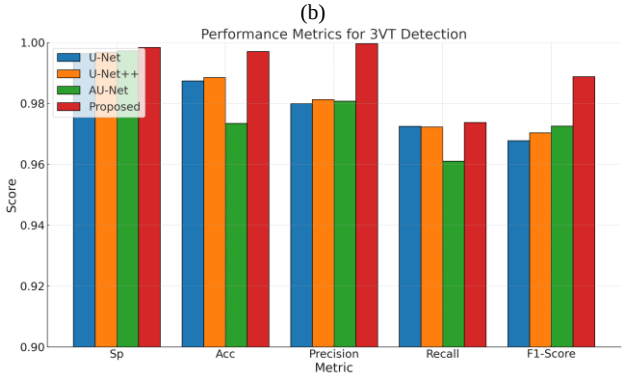

(c)

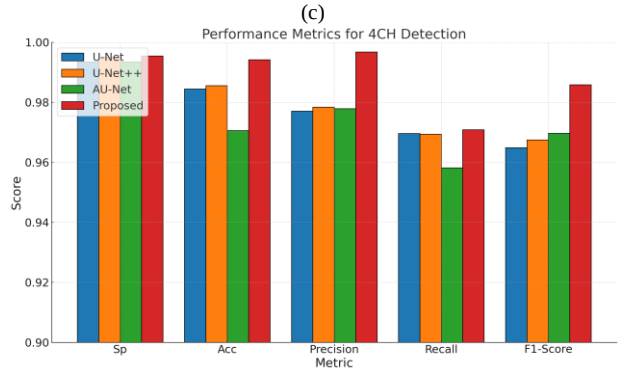

(d)

Fig. 4. (a) Performance for LVOT, (b) Performance for RVOT, (c) Performance for 3VT and (d) Performance for 4CH.

In the RVOT assessment in Fig. 4(b), the U-Net delivered a specificity of 99.4%, accuracy of 98.5%, precision at 97.76%, recall of 97.01%, and an F1-score of 96.54%. The U-Net++ showed improvement, especially in specificity (99.55%) and accuracy (98.61%), with precision slightly higher at 97.89%, nearly similar recall (96.99%), and an F1-score of 96.8%. The AU-Net matched U-Net's specificity but had lower accuracy (97.11%), precision (97.84%), and a recall of 95.87%, leading to an F1-score of 97.02%. The proposed model notably outshined others with a specificity of 99.6%, accuracy reaching 99.47%, precision at an impressive 99.73%, recall of 97.14%, and the highest F1-score of 98.64%, indicating superior performance in FCR detection. For the 3VT view, the U-Net's metrics were vital, with a specificity of 99.64%, accuracy of 98.74%, and precision at 98%, accompanied by a recall of 97.25% and an F1-score of 96.78%. The U-Net++ edged out slightly higher in specificity (99.69%) and accuracy (98.85%), with precision at 98.13%, a comparable recall of 97.23%, and an F1-score of 97.04%. The AU-Net model surpassed U-Net++ in specificity (99.73%) but lagged in accuracy (97.35%), with precision almost equivalent to U-Net++ (98.08%), a lower recall of 96.11% and an F1-score of 97.26%. Remarkably, the proposed model excelled with the highest specificity (99.84%), almost perfect accuracy (99.71%), precision nearly reaching 100% (99.97%), recall of 97.38%, and an F1-score of 98.88%, demonstrating unmatched efficacy in detecting FCR in the 3VT view as shown in Fig. 4(c)

The U-Net model exhibits solid performance with a specificity of 99.35%, an accuracy of 98.45%, precision at 97.71%, recall of 96.96%, and an F1-score of 96.49%. U-Net++ improves upon U-Net's metrics slightly, achieving a specificity of 99.5%, an accuracy of 98.56%, and a precision of 97.84%. The recall, at 96.94%, is marginally lower than U-Net's, but it achieves a higher F1-score of 96.75%, indicating a better balance between precision and recall. While maintaining the same specificity as U-Net at 99.35%, AU-Net decreases accuracy to 97.06%. However, its precision remains high at 97.79%, with a recall of 95.82% and an F1-score of 96.97%. This proposes that AU-Net, despite its slightly lower accuracy and recall, remains competitive in precision and overall F1 score. The proposed model stands out significantly among the evaluated models, showcasing this group's highest specificity (99.55%) and accuracy (99.42%). With precision reaching 99.68% and recall at 97.09%, it achieves an F1-score of 98.59%. These figures indicate a superior ability to detect and diagnose FCR in the 4CH view accurately (see Fig. 4(d)), reducing false positives (as evidenced by the high precision) while still correctly identifying a high percentage of true positive cases (as shown by the recall).

Throughout the training and validation phases (Fig. 5 (a)) and (b)), the evolution of training and validation losses for U-Net, U-Net++, AU-Net, and the proposed model illuminates the unique learning dynamics and generalization capabilities inherent to each architecture. Initially, the U-Net model faced significant challenges, which was evident from its high training loss of 0.6000. In contrast, U-Net++ and AU-Net kick off with lower initial training losses (0.3830 and 0.3603, respectively), hinting at their advanced architectures' capacity for a more refined initial understanding of the data complexities. Remarkably, the proposed model begins with the lowest training loss at 0.2652, signalling a practical grasp of the ECGc image patterns for Fetal Cardiac Rhabdomyoma detection right from the start. As all the models progress through the epochs, they all exhibit a declining trend in terms of training loss, which is indicative of learning and refinement. The proposed model was

better because it maintained the lowest loss throughout the training, which at last resulted in a final training loss of 0.0057. This shows superior performance and high accuracy potential in medical image segmentation tasks. The AU-Net, however, has an increased initial validation loss and drops to the rest of the models that participate in the validation loss analysis, which concludes in a validation loss of 0.0246. This proceeds simultaneously with the analysis and review of validation loss. This proves that the proposed approach possesses significant learning and adaptation features, which sets it against other comparable models.

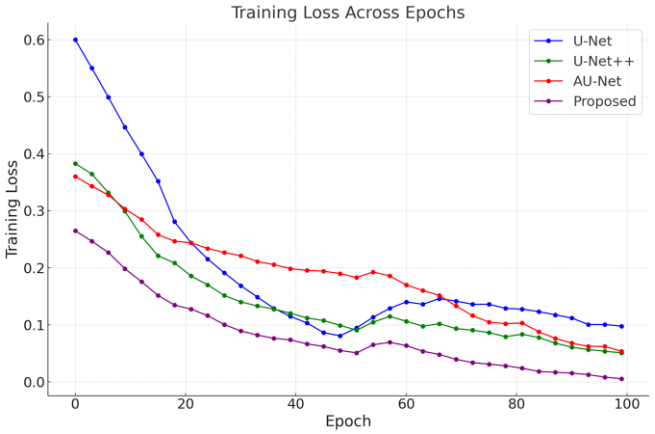

(a)

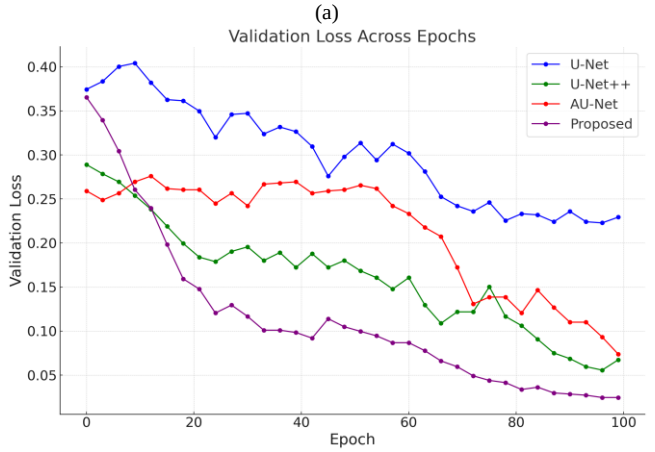

(b)

Fig. 5. (a) Training loss vs. epochs and (b) Validation loss vs. epochs.

VI. Conclusion

In the continuously evolving field of health care tests, the techniques of employing deep learning (DL) technologies when necessary for the detection of Foetal Cardiac Rhabdomyoma (FCR) from echocardiographic (ECG) images are growing into exciting new possibilities of techniques for addressing complicated medical problems. Such techniques have the possibility of helping determine the cause of foetal heart disease. The intricate nature of foetal cardiovascular anatomy and the drawbacks of currently available diagnostic techniques make accurate detection of the FCR, a more frequently occurring newborn illness, challenging. Several currently available CNN models have demonstrated significant success in medical image segmentation; these comprise the initially developed U-Net and versions such as U-Net++ and AU-Net. The issue with these techniques is that they frequently fail to attempt to collect the subtle features that are necessary for FCR detection, as demonstrated by experiments. This might be because the model fails to represent the degree of detail needed for accurate diagnostics properly, and the scale is similar across layers. The present research introduces the attention-calibrated U-Net (ACU-Net), an enhanced form of U-Net that merges attention mechanisms with the original version of U-Net to deal with those problems. The ACU-Net uses the proposed hybrid loss function, which incorporates cross-entropy loss, dice loss, and attention-driven components. The objective is to make the algorithm more successful in segmenting FCR from ECG images regarding attention, accuracy, and cost.

Employing the sourced ECG dataset results from experiments demonstrated that the recommended ACU-Net performed more effectively than U-Net and its different versions models in detecting FCR across multiple performance metrics analysis, including specificity, accuracy, precision, recall, and F1-score.

References

[1] Siddique, N., Paheding, S., Elkin, C. P., & Devabhaktuni, V. (2021). U-net and its variants for medical image segmentation: A review of theory and applications. IEEE Access, 9, 82031-82057.

[2] Zhou, Z., Rahman Siddiquee, M. M., Tajbakhsh, N., & Liang, J. (2018). Unet++: A nested u-net architecture for medical image segmentation. In *Deep Learning in Medical Image Analysis and Multimodal Learning for Clinical Decision Support: 4th International Workshop, DLMIA 2018, and 8th International Workshop, ML-CDS 2018, Held in Conjunction with MICCAI 2018, Granada, Spain, September 20, 2018, Proceedings 4* (pp. 3-11). Springer International Publishing.

[3] Oktay, O., et al., (2018). Attention u-net: Learning where to look for the pancreas. *arXiv preprint arXiv:1804.03999*.

[4] Zhang, S., & Zhang, C. (2023). Modified U-Net for plant-diseased leaf image segmentation. *Computers and Electronics in Agriculture*, *204*, 107511.

[5] Yin, L., et al., (2023). U-Net-STN: A novel end-to-end lake boundary prediction model. *Land*, *12*(8), 1602.

[6] Allah, A. M. G., Sarhan, A. M., & Elshennawy, N. M. (2023). Edge U-Net: Brain tumor segmentation using MRI based on deep U-Net model with boundary information. *Expert Systems with Applications*, *213*, 118833.

[7] Bougourzi, F., Distante, C., Dornaika, F., & Taleb-Ahmed, A. (2023). PDAtt-Unet: Pyramid dual-decoder attention Unet for COVID-19 infection segmentation from CT scans. *Medical Image Analysis*, *86*, 102797.

[8] Zhang, J., Qin, Q., Ye, Q., & Ruan, T. (2023). ST-unit: Swin transformer boosted U-net with cross-layer feature enhancement for medical image segmentation—*computers in Biology and Medicine*, *153*, 106516.

[9] Ruan, J., Xie, M., Gao, J., Liu, T., & Fu, Y. (2023). Ege-unit: an efficient group enhanced unet for skin lesion segmentation. *International Conference on Medical Image Computing and Computer-Assisted Intervention* (pp. 481-490). Cham: Springer Nature Switzerland.

[10] Aghdam, E. K., Azad, R., Zarvani, M., & Merhof, D. (2023). Attention Swin u-net: Cross-contextual attention mechanism for skin lesion segmentation. *IEEE 20th International Symposium on Biomedical Imaging (ISBI)* (pp. 1-5). IEEE.

[11] D. Jha, M. A. Riegler, D. Johansen, P. Halvorsen and H. D. Johansen, "DoubleU-Net: A Deep Convolutional Neural Network for Medical Image Segmentation," 2020 IEEE 33rd International Symposium on Computer-Based Medical Systems (CBMS), Rochester, MN, USA, 2020, pp. 558-564, doi: 10.1109/CBMS49503.2020.00111.

[12] K. D. Shah, D. K. Patel, M. P. Thaker, H. A. Patel, M. J. Saikia and B. J. Ranger, "EMED-UNet: An Efficient Multi-Encoder-Decoder Based UNet

for Medical Image Segmentation," IEEE Access, vol. 11, pp. 95253-95266, 2023, doi: 10.1109/ACCESS.2023.3309158.

[13] S. S, A. Rafee, M. S. H and V. K. R, "Optimizing Left Atrium Segmentation: A Modified U-NET Architecture with MRI Image Slicing," 2023 IEEE 2nd International Conference on Data, Decision and Systems (ICDDS), Mangaluru, India, 2023, pp. 1-6, doi: 10.1109/ICDDS59137.2023.10434364.

[14] S. Tripathi, R. Wadhwani, A. Rasool and A. Jadhav, "Comparison Analysis of Deep Learning Models In Medical Image Segmentation," 2023 13th International Conference on Cloud Computing, Data Science & Engineering (Confluence), Noida, India, 2023, pp. 468-471, doi: 10.1109/Confluence56041.2023.10048822.

[15] H. H. Yu, X. Feng, Z. Wang and H. Sun, "MixModule: Mixed CNN Kernel Module for Medical Image Segmentation," 2020 IEEE 17th International Symposium on Biomedical Imaging (ISBI), Iowa City, IA, USA, 2020, pp. 1508-1512, doi: 10.1109/ISBI45749.2020.9098498.

[16] Y. Weng, T. Zhou, Y. Li and X. Qiu, "NAS-Unet: Neural Architecture Search for Medical Image Segmentation," in IEEE Access, vol. 7, pp. 44247-44257, 2019, doi: 10.1109/ACCESS.2019.2908991.

[17] A. Bhattacharjya, 'A Holistic Study On The Use Of Blockchain Technology In CPS And IoT Architectures Maintaining The Cia Triad In Data Communication', *International Journal of Applied Mathematics and Computer Science*, vol. 32, no. 3, pp. 403–413, 2022.

[18] 3, 2022.A. H. Elsheikh *et al.*, 'Fine-tuned artificial intelligence model using pigeon optimizer for prediction of residual stresses during turning of Inconel 718', *Journal of Materials Research and Technology*, vol. 15, pp. 3622–3634, 2021.

[19] A. A. Alnuaim *et al.*, 'Human-Computer Interaction for Recognizing Speech Emotions Using Multilayer Perceptron Classifier', *Journal of Healthcare Engineering*, vol. 2022, 2022.

[20] A. Appathurai, R. Sundarasekar, C. Raja, E. J. Alex, C. A. Palagan, and A. Nithya, 'An Efficient Optimal Neural Network-Based Moving Vehicle Detection in Traffic Video Surveillance System', *Circuits, Systems, and Signal Processing*, vol. 39, no. 2, pp. 734–756, 2020.

[21] A. Banchhor and N. Srinivasu, 'Integrating Cuckoo search-Grey wolf optimization and Correlative Naive Bayes classifier with Map Reduce model for big data classification', *Data and Knowledge Engineering*, vol. 127, 2020.

[22] A. H. Elsheikh *et al.*, 'Low-cost bilayered structure for improving the performance of solar stills: Performance/cost analysis and water yield prediction using machine learning', *Sustainable Energy Technologies and Assessments*, vol. 49, 2022.

[23] A. M. Gandhi *et al.*, 'Performance enhancement of stepped basin solar still based on OSELM with traversal tree for higher energy adaptive control', *Desalination*, vol. 502, 2021.

[24] A. M. Gandhi *et al.*, 'SiO2/TiO2 nanolayer synergistically trigger thermal absorption inflammatory responses materials for performance improvement of stepped basin solar stillnatural distiller', *Sustainable Energy Technologies and Assessments*, vol. 52, 2022.

[25] A. Naik and S. C. Satapathy, 'A comparative study of social group optimization with a few recent optimization algorithms', *Complex and Intelligent Systems*, vol. 7, no. 1, pp. 249–295, 2021.

[26] A. Naik, S. C. Satapathy, and A. Abraham, 'Modified Social Group Optimization—a meta-heuristic algorithm to solve short-term hydrothermal scheduling', *Applied Soft Computing Journal*, vol. 95, 2020.

[27] A. O. Alsaiari *et al.*, 'Applications of TiO2/Jackfruit peel nanocomposites in solar still: Experimental analysis and performance evaluation', *Case Studies in Thermal Engineering*, vol. 38, 2022.

[28] A. Ruwali, A. J. S. Kumar, K. B. Prakash, G. Sivavaraprasad, and D. V. Ratnam, 'Implementation of Hybrid Deep Learning Model (LSTM-CNN) for Ionospheric TEC Forecasting Using GPS Data', *IEEE Geoscience and Remote Sensing Letters*, vol. 18, no. 6, pp. 1004–1008, 2021.

[29] A. S. Abdullah *et al.*, 'Enhancing trays solar still performance using wick finned absorber, nano-enhanced PCM', *Alexandria Engineering Journal*, vol. 61, no. 12, pp. 12417–12430, 2022.

[30] A. S. Zamani *et al.*, 'Performance of Machine Learning and Image Processing in Plant Leaf Disease Detection', *Journal of Food Quality*, vol. 2022, 2022.

[31] A. V. N. Reddy, C. P. Krishna, and P. K. Mallick, 'An image classification framework exploring the capabilities of extreme learning machines and artificial bee colony', *Neural Computing and Applications*, vol. 32, no. 8, pp. 3079–3099, 2020.

[32] A. Yadav, S. Chatterjee, and S. M. Equeenuddin, 'Suspended sediment yield modeling in Mahanadi River, India by multi-objective optimization hybridizing artificial intelligence algorithms', *International Journal of Sediment Research*, vol. 36, no. 1, pp. 76–91, 2021.

[33] B. Abi *et al.*, 'Neutrino interaction classification with a convolutional neural network in the DUNE far detector', *Physical Review D*, vol. 102, no. 9, 2020.

[34] B. Acharjya and S. Das, 'Adoption of E-Learning During the COVID-19 Pandemic: The Moderating Role of Age and Gender', *International Journal of Web-Based Learning and Teaching Technologies*, vol. 17, no. 2, 2022.

[35] C. Banchhor and N. Srinivasu, 'Integrating Cuckoo search-Grey wolf optimization and Correlative Naive Bayes classifier with Map Reduce model for big data classification', *Data and Knowledge Engineering*, vol. 127, 2020.

[36] C. Sridhar, P. K. Pareek, R. Kalidoss, S. S. Jamal, P. K. Shukla, and S. J. Nuagah, 'Optimal Medical Image Size Reduction Model Creation Using Recurrent Neural Network and GenPSOWVQ', *Journal of Healthcare Engineering*, vol. 2022, 2022.

[37] D. B. V, S. P. Kodali, and N. R. Boggarapu, 'Multi-objective optimization for optimum abrasive water jet machining process parameters of Inconel718 adopting the Taguchi approach', *Multidiscipline Modeling in Materials and Structures*, vol. 16, no. 2, pp. 306–321, 2020.

[38] D. Balamurugan, S. S. Aravinth, P. C. S. Reddy, A. Rupani, and A. Manikandan, 'Multiview Objects Recognition Using Deep Learning-Based Wrap-CNN with Voting Scheme', *Neural Processing Letters*, vol. 54, no. 3, pp. 1495–1521, 2022.

[39] D. Bhattacharyya, B. P. Doppala, and N. Thirupathi Rao, 'Prediction and forecasting of persistent kidney problems using machine learning algorithms', *International Journal of Current Research and Review*, vol. 12, no. 20, pp. 134–139, 2020.

[40] D. Bhavana, K. Kishore Kumar, M. B. Chandra, P. V. Sai Krishna Bhargav, D. Joy Sanjana, and G. Mohan Gopi, 'Hand sign recognition using CNN', *International Journal of Performability Engineering*, vol. 17, no. 3, pp. 314–321, 2021.

[41] D. P. Yadav, A. Sharma, S. Athithan, A. Bhola, B. Sharma, and I. B. Dhaou, 'Hybrid SFNet Model for Bone Fracture Detection and Classification Using ML/DL', *Sensors*, vol. 22, no. 15, 2022.

[42] E. I. Ghandourah *et al.*, 'Performance assessment of a novel solar distiller with a double slope basin covered by coated wick with lanthanum cobalt oxide nanoparticles', *Case Studies in Thermal Engineering*, vol. 32, 2022.

[43] E. K. Kumar, P. V. V. Kishore, M. T. Kiran Kumar, and D. A. Kumar, '3D sign language recognition with joint distance and angular coded color topographical descriptor on a 2 – stream CNN', *Neurocomputing*, vol. 372, pp. 40–54, 2020.

[44] E. Rajesh Kumar, K. V. S. N. Rama Rao, S. R. Nayak, and R. Chandra, 'Suicidal ideation prediction in twitter data using machine learning techniques', *Journal of Interdisciplinary Mathematics*, vol. 23, no. 1, pp. 117–125, 2020.

[45] E. S. N. Joshua, D. Bhattacharyya, M. Chakkravarthy, and H.-J. Kim, 'Lung cancer classification using squeeze and excitation convolutional neural networks with grad Cam++ class activation function', *Traitement du Signal*, vol. 38, no. 4, pp. 1103–1112, 2021.

[46] E. S. Neal Joshua, D. Bhattacharyya, M. Chakkravarthy, and Y.-C. Byun, '3D CNN with Visual Insights for Early Detection of Lung Cancer Using Gradient-Weighted Class Activation', *Journal of Healthcare Engineering*, vol. 2021, 2021.

[47] E. S. Neal Joshua, M. Chakkravarthy, and D. Bhattacharyya, 'An extensive review on lung cancer detection using machine learning techniques: A systematic study', *Revue d'Intelligence Artificielle*, vol. 34, no. 3, pp. 351–359, 2020.

[48] G. Ramkumar, R. Thandaiah Prabu, N. Phalguni Singh, and U. Maheswaran, 'Experimental analysis of brain tumor detection system using Machine learning approach', *Materials Today: Proceedings*, 2021.

[49] I. Lakshmi Mallika, D. Venkata Ratnam, S. Raman, and G. Sivavaraprasad, 'A New Ionospheric Model for Single Frequency GNSS User Applications Using Klobuchar Model Driven by Auto Regressive Moving Average (SAKARMA) Method over Indian Region', *IEEE Access*, vol. 8, pp. 54535–54553, 2020.

[50] J. R. K. K. Dabbakuti, A. Jacob, V. R. Veeravalli, and R. K. Kallakunta, 'Implementation of IoT analytics ionospheric forecasting system based on machine learning and ThingSpeak', *IET Radar, Sonar and Navigation*, vol. 14, no. 2, pp. 341–347, 2020.

[51] J. R. Reddy, A. Pandian, and C. R. Reddy, 'An efficient learning based RFMFA technique for islanding detection scheme in distributed generation systems', *Applied Soft Computing Journal*, vol. 96, 2020.

[52] K. K. D. Ramesh, G. Kiran Kumar, K. Swapna, D. Datta, and S. Suman Rajest, 'A review of medical image segmentation algorithms', *EAI Endorsed Transactions on Pervasive Health and Technology*, vol. 7, no. 27, 2021.

[53] K. K. D. Ramesh, G. Kiran Kumar, K. Swapna, D. Datta, and S. Suman Rajest, 'A review of medical image segmentation algorithms', *EAI Endorsed Transactions on Pervasive Health and Technology*, vol. 7, no. 27, 2021.

[54] K. Mannepalli, P. N. Sastry, and M. Suman, 'Emotion recognition in speech signals using optimization based multi-SVNN classifier', *Journal of King Saud University - Computer and Information Sciences*, vol. 34, no. 2, pp. 384–397, 2022.

[55] K. N. Dattatraya and K. R. Rao, 'Hybrid based cluster head selection for maximizing network lifetime and energy efficiency in WSN', *Journal of King Saud University - Computer and Information Sciences*, vol. 34, no. 3, pp. 716–726, 2022.

[56] K. Raju *et al.*, 'A robust and accurate video watermarking system based on svd hybridation for performance assessment', *International Journal of Engineering Trends and Technology*, vol. 68, no. 7, pp. 19–24, 2020.

[57] K. Saikumar and V. Rajesh, 'A novel implementation heart diagnosis system based on random forest machine learning technique', *International Journal of Pharmaceutical Research*, vol. 12, pp. 3904–3916, 2020.

[58] K. Saikumar, V. Rajesh, and B. S. Babu, 'Heart Disease Detection Based on Feature Fusion Technique with Augmented Classification Using Deep Learning Technology', *Traitement du Signal*, vol. 39, no. 1, pp. 31–42, 2022.

[59] K. Thirugnanasambandam, M. Rajeswari, D. Bhattacharyya, and J.-Y. Kim, 'Directed Artificial Bee Colony algorithm with revamped search strategy to solve global numerical optimization problems', *Automated Software Engineering*, vol. 29, no. 1, 2022.

[60] L. Goswami *et al.*, 'A critical review on prospects of bio-refinery products from second and third generation biomasses', *Chemical Engineering Journal*, vol. 448, 2022.

[61] L. Mallika I, D. V. Ratnam, S. Raman, and G. Sivavaraprasad, 'Machine learning algorithm to forecast ionospheric time delays using Global Navigation satellite system observations', *Acta Astronautica*, vol. 173, pp. 221–231, 2020.

[62] M. A. A. Al-qaness *et al.*, 'Efficient artificial intelligence forecasting models for COVID-19 outbreak in Russia and Brazil', *Process Safety and Environmental Protection*, vol. 149, pp. 399–409, 2021.

[63] M. Baskar, J. Ramkumar, C. Karthikeyan, V. Anbarasu, A. Balaji, and T. S. Arulananth, 'Low rate DDoS mitigation using real-time multi threshold traffic monitoring system', *Journal of Ambient Intelligence and Humanized Computing*, 2021.

[64] M. K. Thota, F. H. Shajin, and P. Rajesh, 'Survey on software defect prediction techniques', *International Journal of Applied Science and Engineering*, vol. 17, no. 4, pp. 331–344, 2020.

[65] M. Mohammed, R. Kolapalli, N. Golla, and S. S. Maturi, 'Prediction of rainfall using machine learning techniques', *International Journal of Scientific and Technology Research*, vol. 9, no. 1, pp. 3236–3240, 2020.

[66] M. S. Mekala and P. Viswanathan, '(t,n): Sensor Stipulation with THAM Index for Smart Agriculture Decision-Making IoT System', *Wireless Personal Communications*, vol. 111, no. 3, pp. 1909–1940, 2020.

[67] M. Y. B. Murthy, A. Koteswararao, and M. S. Babu, 'Adaptive fuzzy deformable fusion and optimized CNN with ensemble classification for automated brain tumor diagnosis', *Biomedical Engineering Letters*, vol. 12, no. 1, pp. 37–58, 2022.

[68] M. Z. U. Rahman, S. Surekha, K. P. Satamraju, S. S. Mirza, and A. Lay-Ekuakille, 'A Collateral Sensor Data Sharing Framework for Decentralized Healthcare Systems', *IEEE Sensors Journal*, vol. 21, no. 24, pp. 27848–27857, 2021.

[69] N. Satheesh *et al.*, 'Flow-based anomaly intrusion detection using machine learning model with software defined networking for OpenFlow network', *Microprocessors and Microsystems*, vol. 79, 2020.

[70] N. Satheesh *et al.*, 'Flow-based anomaly intrusion detection using machine learning model with software defined networking for OpenFlow network', *Microprocessors and Microsystems*, vol. 79, 2020.

[71] N. V. Kimmatkar and B. Vijaya Babu, 'Novel approach for emotion detection and stabilizing mental state by using machine learning techniques', *Computers*, vol. 10, no. 3, 2021.

[72] N. V. Rani and K. Ravindhranath, 'PEG-400 promoted a simple, efficient and eco-friendly synthesis of functionalized novel isoxazolyl pyrido[2,3-d]pyrimidines and their antimicrobial and anti-inflammatory activity', *Synthetic Communications*, vol. 51, no. 8, pp. 1171–1183, 2021.

[73] N. Yuvaraj, K. Praghash, R. A. Raja, and T. Karthikeyan, 'An Investigation of Garbage Disposal Electric Vehicles (GDEVs) Integrated with Deep Neural Networking (DNN) and Intelligent Transportation System (ITS) in Smart City Management System (SCMS)', *Wireless Personal Communications*, vol. 123, no. 2, pp. 1733–1752, 2022.

[74] N. Yuvaraj, T. Karthikeyan, and K. Praghash, 'An Improved Task Allocation Scheme in Serverless Computing Using Gray Wolf Optimization (GWO) Based Reinforcement Learning (RIL) Approach', *Wireless Personal Communications*, vol. 117, no. 3, pp. 2403–2421, 2021.

[75] Naik, S. C. Satapathy, and A. Abraham, 'Modified Social Group Optimization—a meta-heuristic algorithm to solve short-term hydrothermal scheduling', *Applied Soft Computing Journal*, vol. 95, 2020.

[76] P. Chithaluru, F. Al-Turjman, T. Stephan, M. Kumar, and L. Mostarda, 'Energy-efficient blockchain implementation for Cognitive Wireless Communication Networks (CWCNs)', *Energy Reports*, vol. 7, pp. 8277–8286, 2021.

[77] P. K. Pareek *et al.*, 'IntOPMICM: Intelligent Medical Image Size Reduction Model', *Journal of Healthcare Engineering*, vol. 2022, 2022.

[78] P. Sharma, N. R. Moparthi, S. Namasudra, V. Shanmuganathan, and C.-H. Hsu, 'Blockchain-based IoT architecture to secure healthcare system using identity-based encryption', *Expert Systems*, vol. 39, no. 10, 2022.

[79] R. Janarthanan, R. U. Maheshwari, P. K. Shukla, P. K. Shukla, S. Mirjalili, and M. Kumar, 'Intelligent detection of the PV faults based on artificial neural network and type 2 fuzzy systems', *Energies*, vol. 14, no. 20, 2021.

[80] R. K. Mojjada, A. Yadav, A. V. Prabhu, and Y. Natarajan, 'Machine learning models for covid-19 future forecasting', *Materials Today: Proceedings*, 2021.

[81] S. C. Dharmadhikari, V. Gampala, C. M. Rao, S. Khasim, S. Jain, and R. Bhaskaran, 'A smart grid incorporated with ML and IoT for a secure management system', *Microprocessors and Microsystems*, vol. 83, 2021.

[82] S. D. M. Achanta, T. Karthikeyan, and R. Vinoth Kanna, 'A wireless IOT system towards gait detection technique using FSR sensor and wearable IoT devices', *International Journal of Intelligent Unmanned Systems*, vol. 8, no. 1, pp. 43–54, 2020.

[83] S. Deshmukh, K. Thirupathi Rao, and M. Shabaz, 'Collaborative Learning Based Straggler Prevention in Large-Scale Distributed Computing Framework', *Security and Communication Networks*, vol. 2021, 2021.

[84] S. H. Ahammad, V. Rajesh, M. Z. U. Rahman, and A. Lay-Ekuakille, 'A Hybrid CNN-Based Segmentation and Boosting Classifier for Real Time Sensor Spinal Cord Injury Data', *IEEE Sensors Journal*, vol. 20, no. 17, pp. 10092–10101, 2020.

[85] S. Hira, A. Bai, and S. Hira, 'An automatic approach based on CNN architecture to detect Covid-19 disease from chest X-ray images', *Applied Intelligence*, vol. 51, no. 5, pp. 2864–2889, 2021.

[86] S. Joshi *et al.*, 'Unified Authentication and Access Control for Future Mobile Communication-Based Lightweight IoT Systems Using

Blockchain', *Wireless Communications and Mobile Computing*, vol. 2021, 2021.

[87] S. K. Kalagotla, S. V. Gangashetty, and K. Giridhar, 'A novel stacking technique for prediction of diabetes', *Computers in Biology and Medicine*, vol. 135, 2021.

[88] S. Kailasam, S. D. M. Achanta, P. Rama Koteswara Rao, R. Vatambeti, and S. Kayam, 'An IoT-based agriculture maintenance using pervasive computing with machine learning technique', *International Journal of Intelligent Computing and Cybernetics*, vol. 15, no. 2, pp. 184–197, 2022.

[89] S. Kumar, A. Jain, A. Kumar Agarwal, S. Rani, and A. Ghimire, 'Object-Based Image Retrieval Using the U-Net-Based Neural Network', *Computational Intelligence and Neuroscience*, vol. 2021, 2021.

[90] S. Mishra, L. Jena, H. K. Tripathy, and T. Gaber, 'Prioritized and predictive intelligence of things enabled waste management model in smart and sustainable environment', *PLoS ONE*, vol. 17, no. 8 August, 2022.

[91] S. N. J. Eali, D. Bhattacharyya, T. R. Nakka, and S.-P. Hong, 'A Novel Approach in Bio-Medical Image Segmentation for Analyzing Brain Cancer Images with U-NET Semantic Segmentation and TPLD Models Using SVM', *Traitement du Signal*, vol. 39, no. 2, pp. 419–430, 2022.

[92] S. Namasudra, R. Chakraborty, A. Majumder, and N. R. Moparthi, 'Securing Multimedia by Using DNA-Based Encryption in the Cloud Computing Environment', *ACM Transactions on Multimedia Computing, Communications and Applications*, vol. 16, no. 3s, 2021.

[93] S. P. Jaiprakash, M. B. Desai, C. S. Prakash, V. H. Mistry, and K. L. Radadiya, 'Low dimensional DCT and DWT feature based model for detection of image splicing and copy-move forgery', *Multimedia Tools and Applications*, vol. 79, no. 39–40, pp. 29977–30005, 2020.

[94] S. R. Dasari, S. Tondepu, L. R. Vadali, and N. Seelam, 'PEG-400 mediated an efficient eco-friendly synthesis of new isoxazolyl pyrido[2,3-d]pyrimidines and their anti-inflammatory and analgesic activity', *Synthetic Communications*, pp. 2950–2961, 2020.

[95] S. Rajasoundaran *et al.*, 'Machine learning based deep job exploration and secure transactions in virtual private cloud systems', *Computers and Security*, vol. 109, 2021.

[96] S. Rajasoundaran *et al.*, 'Secure routing with multi-watchdog construction using deep particle convolutional model for IoT based 5G wireless sensor networks', *Computer Communications*, vol. 187, pp. 71–82, 2022.

[97] S. Rajasoundaran *et al.*, 'Secure watchdog selection using intelligent key management in wireless sensor networks', *Materials Today: Proceedings*, 2021.

[98] S. Rani, D. Ghai, S. Kumar, M. V. V. P. Kantipudi, A. H. Alharbi, and M. A. Ullah, 'Efficient 3D AlexNet Architecture for Object Recognition Using Syntactic Patterns from Medical Images', *Computational Intelligence and Neuroscience*, vol. 2022, 2022.

[99] S. Routray, P. P. Malla, S. K. Sharma, S. K. Panda, and G. Palai, 'A new image denoising framework using bilateral filtering based non-subsampled shearlet transform', *Optik*, vol. 216, 2020.

[100] S. S. Saba, D. Sreelakshmi, P. Sampath Kumar, K. Sai Kumar, and S. R. Saba, 'Logistic regression machine learning algorithm on MRI brain image for fast and accurate diagnosis', *International Journal of Scientific and Technology Research*, vol. 9, no. 3, pp. 7076–7081, 2020.

[101] S. Sekar *et al.*, 'Autonomous Transaction Model for E-Commerce Management Using Blockchain Technology', *International Journal of Information Technology and Web Engineering*, vol. 17, no. 1, 2022.

[102] S. Sengan, G. R. K. Rao, O. I. Khalaf, and M. R. Babu, 'Markov mathematical analysis for comprehensive real-time data-driven in healthcare', *Mathematics in Engineering, Science and Aerospace*, vol. 12, no. 1, pp. 77–94, 2021.

[103] S. Sengan, O. I. Khalaf, P. Vidya Sagar, D. K. Sharma, L. Arokia Jesu Prabhu, and A. A. Hamad, 'Secured and privacy-based IDS for healthcare systems on e-medical data using machine learning approach', *International Journal of Reliable and Quality E-Healthcare*, vol. 11, no. 3, 2022.

[104] S. Sengan, P. Vidya Sagar, R. Ramesh, O. I. Khalaf, and R. Dhanapal, 'The optimization of reconfigured real-time datasets for improving classification performance of machine learning algorithms', *Mathematics in Engineering, Science and Aerospace*, vol. 12, no. 1, pp. 43–54, 2021.

[105] S. Stalin *et al.*, 'A Machine Learning-Based Big EEG Data Artifact Detection and Wavelet-Based Removal: An Empirical Approach', *Mathematical Problems in Engineering*, vol. 2021, 2021.

[106] S. Stalin *et al.*, 'A Machine Learning-Based Big EEG Data Artifact Detection and Wavelet-Based Removal: An Empirical Approach', *Mathematical Problems in Engineering*, vol. 2021, 2021.

[107] Sridhar, P. K. Pareek, R. Kalidoss, S. S. Jamal, P. K. Shukla, and S. J. Nuagah, 'Optimal Medical Image Size Reduction Model Creation Using Recurrent Neural Network and GenPSOWVQ', *Journal of Healthcare Engineering*, vol. 2022, 2022.

[108] T. Chakravorti and P. Satyanarayana, 'Non-linear system identification using kernel based exponentially extended random vector functional link network', *Applied Soft Computing Journal*, vol. 89, 2020.

[109] T. Kavitha *et al.*, 'Deep Learning Based Capsule Neural Network Model for Breast Cancer Diagnosis Using Mammogram Images', *Interdisciplinary Sciences – Computational Life Sciences*, vol. 14, no. 1, pp. 113–129, 2022.

[110] U. Bhimavarapu and G. Battineni, 'Skin Lesion Analysis for Melanoma Detection Using the Novel Deep Learning Model Fuzzy GC-SCNN', *Healthcare (Switzerland)*, vol. 10, no. 5, 2022.

[111] U. K. Singh, M. Jamei, M. Karbasi, A. Malik, and M. Pandey, 'Application of a modern multi-level ensemble approach for the estimation of critical shear stress in cohesive sediment mixture', *Journal of Hydrology*, vol. 607, 2022.

[112] V. Bandi, D. Bhattacharyya, and D. Midhunchakkravarthy, 'Prediction of brain stroke severity using machine learning', *Revue d'Intelligence Artificielle*, vol. 34, no. 6, pp. 753–761, 2020.

[113] V. Kumar *et al.*, 'Addressing Binary Classification over Class Imbalanced Clinical Datasets Using Computationally Intelligent Techniques', *Healthcare (Switzerland)*, vol. 10, no. 7, 2022.

[114] V. Kumar *et al.*, 'Addressing Binary Classification over Class Imbalanced Clinical Datasets Using Computationally Intelligent Techniques', *Healthcare (Switzerland)*, vol. 10, no. 7, 2022.

[115] V. N. Mandhala, D. Bhattacharyya, B. Vamsi, and N. Thirupathi Rao, 'Object detection using machine learning for visually impaired people', *International Journal of Current Research and Review*, vol. 12, no. 20, pp. 157–167, 2020.

[116] V. N. Reddy, C. P. Krishna, and P. K. Mallick, 'An image classification framework exploring the capabilities of extreme learning machines and artificial bee colony', *Neural Computing and Applications*, vol. 32, no. 8, pp. 3079–3099, 2020.